Tellus (2007), 59B, 381–386
Printed in Singapore. All rights reserved

TELLUS

Measurements of aerosol particle dry deposition velocity using the relaxed eddy accumulation technique

By TIIA GRÖNHOLM[1]*, PASI P. AALTO[1], VEIJO HILTUNEN[1], ÜLLAR RANNIK[1], JANNE RINNE[1], LAURI LAAKSO[1], SAARA HYVÖNEN[2], TIMO VESALA[1] and MARKKU KULMALA[1], [1]*Department of Physical Sciences, University of Helsinki, Finland;* [2]*Department of Computer Science, University of Helsinki, Finland*

Manuscript received 10 May 2006; in final form 11 December 2006

ABSTRACT

The continuous measurements of aerosol particle deposition velocity have been performed from January 2004 to January 2005 using a REA technique with dynamic deadband. We measured aerosol particle deposition velocity in the size range of 10–150 nanometer with 5–10 nanometer steps using differential mobility analyser for sizing. We were able to measure two size classes simultaneously. One size class was changed at one month intervals, another we kept constant at 30 nm to investigate the effect of seasonal and meteorological variation on deposition velocity. We found that the 80–100 nanometer size particles had the lowest deposition velocity, about 0.4 cm s^{-1}. Deposition velocity increased with decreasing or increasing particle diameter from 80–100 nanometer size. We also found that deposition velocity increases as a function of friction velocity.

1. Introduction

The atmospheric aerosol consists of particles that range widely in size from nanometers to tens of micrometers. When studying the atmospheric aerosol particles, it is important to know the dynamics of the particles: formation, growth and removal processes.

Main removal processes for all particles are wet and dry deposition (Slinn, 1977; Sehmel, 1980). However, a large fraction of nucleation and Aitken mode particles are removed from the atmosphere via a two phase process: first particles grow to larger sizes due to coagulation and next they are removed from the atmosphere by dry or wet deposition. Both wet and dry deposition are size specific (Seinfeld and Pandis, 1998; Laakso et al., 2003). In particular, dry deposition of aerosol particles depends principally on particle size, atmospheric turbulence and stability and the collecting properties of the surface.

In understanding and modelling aerosol dynamics one of the key phenomenon to be better understood is dry deposition. Therefore, measurements of aerosol particle fluxes are crucial. Two micrometeorological techniques have a significant role in flux measurements of trace gases, heat, momentum and aerosol particles. The most direct flux measurement method is the eddy covariance (EC), which requires fast-response sensors. The EC technique is widely used for measurements of carbon dioxide and water fluxes over terrestrial ecosystems. For example, Buzorius et al. (1998) and Held et al. (2006) applied a condensational particle counter (CPC) for flux measurements of aerosol particles greater than 10 nm in diameter by the EC technique. At the same time they measured aerosol particle size distribution and used deposition models to estimate size-dependent deposition velocities of particles.

An alternate method, relaxed eddy accumulation (REA), requires air to be sampled at a constant rate and placed in one container during positive vertical wind velocities (w) and in another during negative w (Businger and Oncley, 1990). Since this method is based on accumulated concentrations, sensors with slower response time are sufficient. REA technique has been used successfully for measurements of fluxes of biogenic volatile organic compounds (Guenther et al., 1996; Haapanala et al., 2006). Gaman et al. (2004) used REA method to measure the atmospheric particle fluxes.

Only few studies of particle fluxes above forest canopies have been conducted and measurements of fluxes of aerosol particles smaller than 100 nm are very scarce (Gallagher et al., 1997; Rannik et al., 2003; Buzorius et al., 1998; Held et al., 2006). Though deposition models exist, they remain unverified due to lack of experimental data (Ruijgrok et al., 1996; Nho-Kim et al., 2004; Zhang et al., 2001). This is especially true for particles below 100 nm in size, where the number concentration is

*Corresponding author.
e-mail: tiia.gronholm@helsinki.fi
DOI: 10.1111/j.1600-0889.2007.00268.x

highest and the impact on atmospheric pollution and public health is substantial. Only few attempts to determine size-segregated deposition velocities for below 100 nm particles exist (Buzorius et al., 2000; Rannik et al., 2001; Held et al., 2006).

We present the analysis of aerosol particle fluxes measured by the REA system. The analysis involves 12 different aerosol particle size classes below 150 nm. Emphasis in our study is on evaluation of size-segregated deposition velocities. This quantity is independent of particle concentration and describes the rate in which particles of certain size are removed from the atmosphere.

2. Methods

The measurements were performed at the SMEAR II station (Station for Measuring Forest Ecosystem–Atmosphere Relations), Hyytiälä, Southern Finland (61°51′N, 24°17′E, 181 m asl). The REA measurement tower is located in a 40-yr-old Scots pine (*Pinus sylvestris* L.) forest with dominant tree height of 14 m. REA measurement level was at 22 m height where the effect of roughness sublayer on turbulence statistics have been observed to be negligible (Rannik et al., 2003). A detailed description of the site, measurements and meteorological studies can be found in Vesala et al. (1998), Rannik (1998) and Kulmala et al. (2001).

Gaman et al. (2004) have developed and tested a REA system for aerosol particle flux measurements. The REA system measures fluxes of particles below 150 nm in diameter size with very narrow size intervals. The system consists of a fast-response sonic anemometer, a flow system, software for operating the valves, and a differential mobility particle sizer (DMPS) for concentration analysis.

The flux (F) is calculated from the measured standard deviation of vertical wind speed (σ_w) and the average concentrations of the species sampled during updrafts ($\overline{C_+}$) and downdrafts ($\overline{C_-}$) by

$$F = \beta\sigma_w(\overline{C_+} - \overline{C_-}), \tag{1}$$

The REA system operates with a varying threshold for valve switching. The threshold is determined by the 5 minutes running mean of σ_w. Such a dynamic deadband, with threshold of $0.5\sigma_w$, made the flux proportionality coefficient (β) independent of observation conditions (Christensen et al., 2000, Gaman et al., 2004). In our measurements, we used constant β, 0.39, calculated from fast-response measurements of temperature T and vertical wind speed w:

$$\beta = \frac{\overline{w'T'}}{\sigma_w(\overline{T_+} - \overline{T_-})}. \tag{2}$$

Average temperatures $\overline{T_+}$ and $\overline{T_-}$ are calculated according to REA principles and $\overline{w'T'}$ is measured covariance between T and w. Gaman et al. (2004) gives more details about the measurement system, β and validation of the system.

The deposition velocity (v_d) is defined by

$$v_d = -\frac{F}{\overline{C}}. \tag{3}$$

where $\overline{C}$ is the average concentration of the particles.

In this study we simultaneously measured two narrow particle size classes. Uncertainties of measured particle sizes depend on DMA transfer function, charging efficiency and the accuracy of flow rates of the DMPS system. By assuming that the maximum uncertainty of flow rates were ±10%, the standard deviation of particle size distribution was between 0.3 nm (for 8 nm particles) and 2.3 nm (for 150 nm particles).

In order to detect the possible seasonal variation we measured flux of the 30 nm size class throughout the measurement period. The other size class we changed at one month intervals. We calculated half-hour average deposition velocities for 30 nm particles using period from March to December (8 months). Mean value was 1.2 and median 1.0 cm s^{-1}. Standard deviation of this period was 1.55 cm s^{-1}. If we now assume that the data were normally distributed we are able to calculate that we need a sample of about 400 half-hour averages for saying with 99% probability that deviation of the sample mean is lower than 0.2 cm s^{-1} from the mean value of whole data. During the one month we get about 500–700 half-hour averages after our data selection described later in this article.

Thus, we assumed that the period of one month was long enough to get statistically significant results for certain size particles. The measurements started on January 2004 with 100 nm and continued from February to January 2005 with 150, 10, 15, 20, 25, 40, 8, 50, 60, 70, 80 and 100 nm size particles.

3. Results and discussion

In order to eliminate dependence on stability, we calculated deposition velocities only from fluxes measured under near-neutral conditions when absolute value of *Obukhov* length $|L|$ was greater than 100. Also, we removed fluxes measured under low turbulence conditions where the u_* was lower than 0.1 m s^{-1} from further analysis. If we consider that w distribution is approximately Gaussian, the fractions of updraft, downdraft and deadband samples should be 31%, 31% and 38%, respectively. In our system median up, down and deadband fractions were about 30%, 30% and 40%, respectively. The difference in proportions to the theoretical ones was probably due to the stochastic nature of turbulence. In our data analysis, we accepted only half-hour averages where the difference between up and down sampling fractions less than 5 percentage units and where the fractions between the median value ±3 percentage units. Also, we discarded data in cases when wind is blowing from the sector of Hyytiälä forestry field station (215°−265°), assumed to be a local anthropogenic particle source.

Figure 1 shows histograms of half an hour deposition velocity values for the 20 nm and 60 nm particles. The shape of the

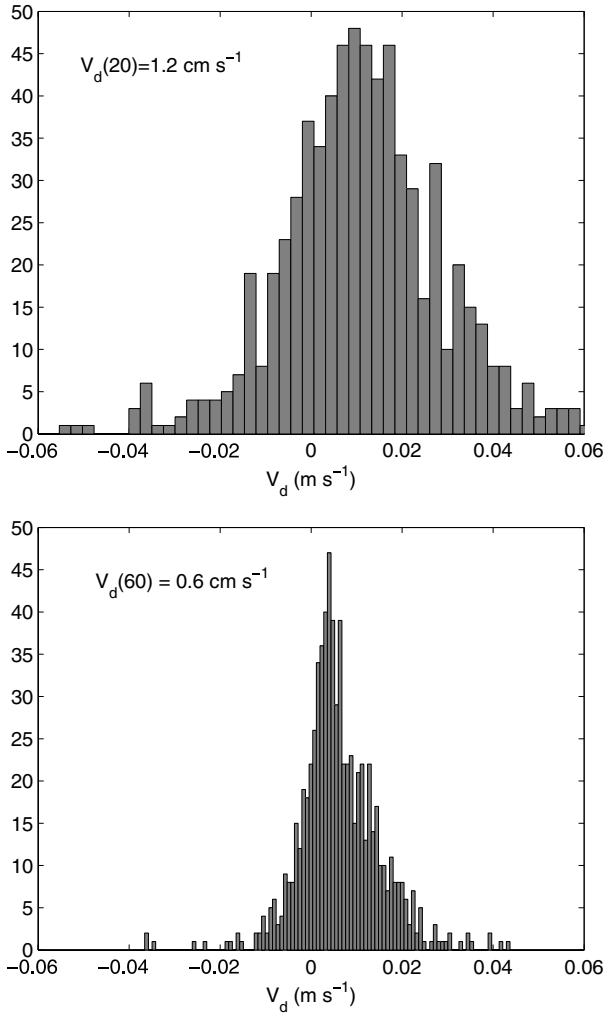

Fig. 1. Histograms of 30 minutes averages of 20 (upper) and 60 nm aerosol particle deposition velocity measurements during one month.

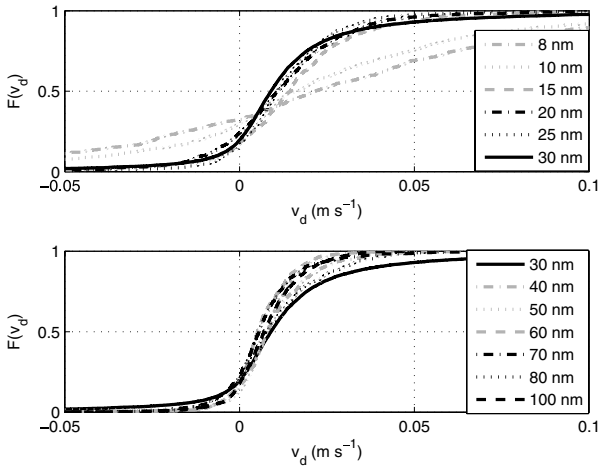

Fig. 2. Cumulative probability distributions of 8–80 nm particle deposition velocities each measured during one month.

distribution was about the same in all cases. Cumulative probability distributions in Figure 2 demonstrates that the distribution of half an hour average deposition velocity values was wide for small sizes and narrowed with increasing particle diameter. This is probably due to lower concentrations of small particles resulting higher random errors in our measurements. The random errors were especially high in the smallest particle sizes, 8 and 10 nm, which result in wide distributions.

The results of deposition velocities obtained by REA system are summarized in Table 1. The results correspond to measurements at 22 m height from January 2004 to January 2005. We present the median deposition velocity value and 25 and 75 percentiles of half-an-hour averages for each size classes. After the data filtering, we had from 381 to 1 089 half-an-hour averages (N) per month, out of 1 440 possible. The percentage of half-an-hour averages indicating deposition varied between 76% and 88%, except in the case of 8 and 10 nm size particles when it was about 70%. For larger than 10 nm particles the fraction of measurements indicating deposition did not correlate with particle size. We believe that most of the occasionally estimates indicating particle emission result from random error in flux values. The average fluxes are significantly different from zero and the standard deviation of 30 minute average values is for all sizes smaller than the average.

The median deposition velocity of continuously measured 30 nm particles were between 0.7–1.0 cm s^{-1} except in September and December 2004 (1.3 and 1.7 cm s^{-1}), and January 2005 (1.7 cm s^{-1}). Figure 3 shows monthly deposition values for 30 nm particles. To avoid the possible seasonal variation of v_d affecting the size resolved v_d we calculated median v_d of 30 nm particles to the whole measurement period ($v_d(30)_{median}$). Then we divided this median by each monthly 30 nm v_d values and used the coefficient to normalize our results. For example, for 20 nm particles the normalized deposition velocity ($v_d(20)_{norm}$) is:

$$v_d(20)_{norm} = \frac{v_d(30)_{median}}{v_d(30)_{20}} v_d(20), \quad (4)$$

where $v_d(30)_{20}$ is the median deposition velocity of 30 nm particles measured at the same period than median deposition velocity of 20 nm particles.

Figure 4 presents v_d of each size class measured and normalized with 30 nm particle median deposition velocity as well as the measurements and parameterization by Gallagher et al. (1997). Vertical bars in our measurements present 25 and, 75 percentiles. According to our measurements the 80–100 nm size particles had the lowest deposition velocities, about 0.4–0.5cm s^{-1}. From 80 to 100 nm size, the deposition velocities increased with decreasing or increasing particle diameter. At the larger end, our results agree with results obtained by Gallagher et al. (1997).

The normalized deposition velocity of 50 nm particles, 0.58 cm s^{-1}, was a slightly higher than 0.48 cm s^{-1} measured by

Table 1. Summary of measurement results. Month refers to measurement period in the year 2004, except the last one, which is measured in January 2005. Size is the diameter of aerosol particle, v_d is the median deposition velocity, v_d/u_* the deposition velocity normalized with friction velocity, 25% and 75% are the percentiles of deposition velocity distribution, median(u_*) is the median value of friction velocity, N is the number of 30 minutes averages used in monthly value calculation, %dep is percentage of observations indicating deposition and $v_d(30)$ is the deposition velocity of 30 nm particles measured during the month in question. v_{dnorm} is the deposition velocity of the size mentioned in column 2 normalized with 30 nm particle median deposition velocity.

Month	Size	v_d	v_d/u_*	25%	75%	N	median(u_*)	%dep	$v_d(30)$	v_{dnorm}
Jan	100	0.69	1.25	1.18	1.06	530	0.48	86	0.95	0.52
Feb	150	0.25	0.32	0.01	0.84	750	0.47	76	0.74	0.56
March	10	1.77	3.11	−0.46	4.41	734	0.56	70	0.72	1.89
April	15	1.49	2.75	0.37	2.46	381	0.49	82	0.78	1.77
May	20	1.18	2.12	0.03	2.21	702	0.56	76	0.87	1.20
June	25	1.23	2.23	0.31	2.08	673	0.51	84	0.89	1.17
July	40	0.94	1.67	0.27	1.53	719	0.55	84	0.86	0.88
Aug	8	2.14	4.21	−1.23	5.81	555	0.39	69	0.96	2.12
Sep	50	0.74	1.31	0.34	1.30	760	0.54	88	1.28	0.58
Oct	60	0.62	1.23	0.15	1.11	733	0.48	81	0.98	0.50
Nov	70	0.66	1.27	0.06	1.14	702	0.49	77	1.06	0.50
Dec	80	0.99	1.49	0.12	1.72	718	0.60	79	1.66	0.44
Jan	100	0.78	1.33	0.18	1.33	1089	0.56	82	1.72	0.38

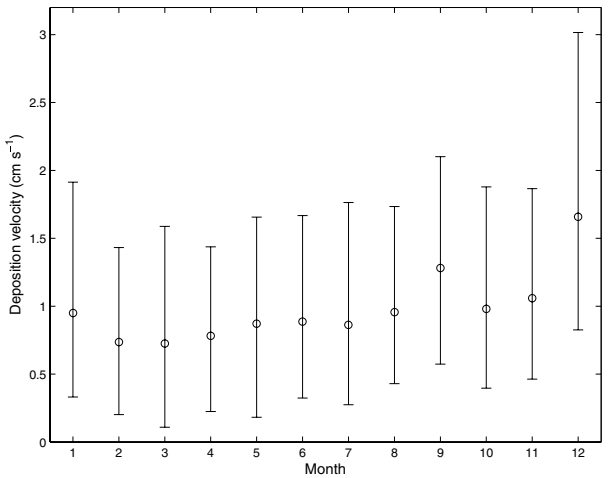

Fig. 3. Dry deposition velocities of 30 nm particles. Circles are the monthly medians calculated from half an hour averages. Vertical bars measurements present 25–75 percentiles.

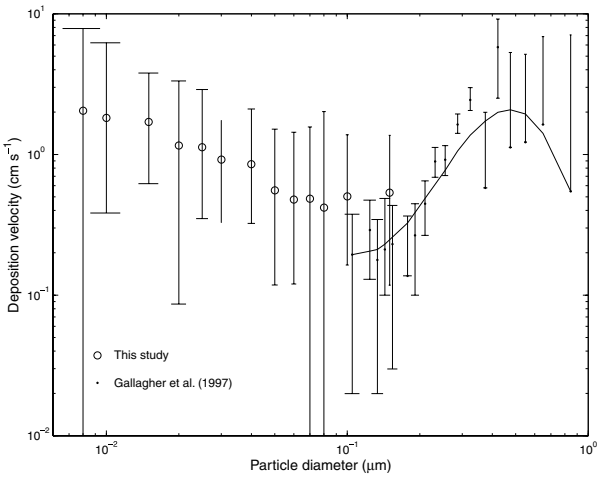

Fig. 4. Dry deposition velocities measured in this study and by Gallagher et al. (1997). Circles present medians of half-an-hour averages and vertical bars in our measurements denote 25 and 75 percentiles.

Gaman et al. (2004). However, when taking uncertainties into account, the results are quite similar. Also, modelled deposition velocities by Held et al. (2006) are similar to our measurements. Rannik et al. (2001) and Buzorius et al. (2000) used EC measurements and determined deposition velocities using flux weighted by size distribution measurements or fitted model to EC data. Their results give a slightly lower deposition velocity values than our measurements.

Figure 5 shows mean deposition velocities of 15–80 nm particles as a function of friction velocity. To get enough data for low and high friction velocities, we combined size classes 15, 20, 25 and 40 nm and size classes 50, 60, 70 and 80 nm. For 30 nm particles, 12 months data were used. Vertical bars denotes standard deviations. Although the uncertainty is large, it seems that a dependence of the deposition velocity on the friction velocity exists, especially for high friction velocity values.

However, in each measuring period, the average meteorological conditions including u_* and horizontal wind speed were about the same. The mean vertical wind speed was between 2.7 and 3.6 m s^{-1} and the mean and median values for u_* were 0.5–0.6 m s^{-1} as can be seen in Table 1. It is possible to normalize

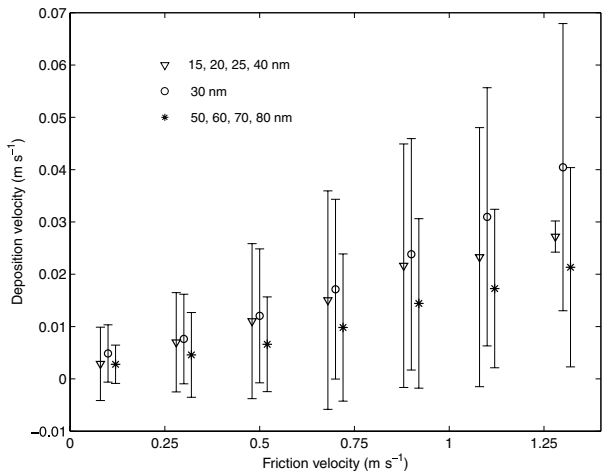

Fig. 5. Dry deposition velocities as a function of friction velocity, mean values and the standard deviations. Size classes 15, 20, 25 and 40 nm are treated together as small particles and 50, 60, 70 and 80 nm are combined for large particles. For particle size 30 nm, 12 months measurement data are utilized.

the half-hour deposition velocities with u_* and calculate the median v_d/u_* instead of v_d. Also the v_d/u_* is presented in Table 1 for each size class. The normalization did not narrow the distributions and the order of magnitude of random errors was the same as for v_d. The explanation for this is that the measured deposition velocity can be considered as

$$v_d = a(u_* + e_{u_*}) + e_{v_d}, \tag{5}$$

where e_{u_*} and e_{v_d} represent independent random errors of friction velocity and deposition velocity, respectively. When we normalize deposition velocity with $u_* + e_{u_*}$ and calculating standard deviations we get

$$std\left(\frac{v_d}{u_* + e_{u_*}}\right) = std\left(\frac{e_{v_d}}{u_* + e_{u_*}}\right) \tag{6}$$

Thus, we can see that when random uncertainty component e_{v_d} is large, then normalization with $u_* < 1$ and frequently <0.4 works as amplification of random error term e_{v_d} and the result is what we obtained. So, there is dependence on u_*, but normalization does not reduce variance because of explanation above.

Despite careful observations, there are several possible processes, that can affect our results. One of the causes of uncertainty is seasonal behaviour of the boreal forest. During the winter (November–March) ground and often also canopy are covered by snow. In contrast, during the summer broad-leafed trees can affect the deposition rates by increasing leaf area in Hyytiälä during the summer. However, as presented in Figure 3, we did not observe clear annual trend. Thus, we may assume that this phenomenon do not lead to any significant bias in our results.

4. Conclusions

In this study, we have carried out aerosol particle flux measurements in a boreal forest environment for 13 months with narrow size intervals. As a main result, we presented experimental deposition velocities calculated from flux measurements for particles between 8 and 150 nm. We used continuously measurements of 30 nm for de-trending the possible effect of seasonal variation to deposition velocities.

Our system was able to measure deposition velocities of 15–150 nm aerosol particles. For sizes of 8 and 10 nm, the random errors dominated the measurements. This is probably due to low particle concentrations and limited counting accuracy. We found lowest deposition velocities, 0.4 cm s^{-1}, for particles in the size range of 80−100 nm. Starting from that size range, deposition velocities increased with increasing or decreasing diameter. Highest deposition velocities ($>$1.7 cm s^{-1}) we detected for below 20 nm particles. As expected, we observed that deposition velocity increases with increasing friction velocity.

To our knowledge, there are only few previous aerosol particle deposition velocity observations with limited number of data points in the size range below 100 nm. Since dry deposition is one of the main removal mechanisms for the particles, our results offer important knowledge on the behaviour of global atmosphere.

5. Acknowledgments

The authors want to thank the two anonymous reviewers for their comments and many helpful suggestions, which improved the paper.

References

Businger, J. A. and Oncley, S. P. 1990. Flux measurement with conditional sampling. *J. Atmos. Oceanic Technol.* **7**, 349–352.

Buzorius, G., Rannik, Ü., Mäkelä, J., Vesala, T. and Kulmala, M. 1998. Vertical aerosol particle fluxes measured by eddy covariance technique using condensational particle counter. *J. Aerosol Sci.* **29**, 157–171.

Buzorius, G., Rannik, Ü., Mäkelä, J. M., Keronen, P., Vesala, T. and co-authors. 2000. Vertical aerosol fluxes measured by eddy covariance method and deposition of nucleation mode particles above a Scots pine forest in southern Finland. *J. Geophys. Res.* **105**, 19905–19916.

Christensen, C. S., Hummelshøj, P., Jensen, N. O., Larsen, B., Lohse, C. and co-authors. 2000. Determination of the terpene flux from orange species and Norway spruce by relaxed eddy accumulation. *Atmos. Environ.* **34**, 3057–3067.

Gallagher, M. W., Beswick, K. M., Duyzer, J., Westrate, H., Choularton, T. W. and co-authors. 1997. Measurements of aerosol fluxes to Speulder forest using a micrometeorological technique. *Atmos. Environ.* **31**, 359–373.

Gaman, A., Rannik, Ü., Aalto, P., Pohja, T., Siivola, E. and co-authors. 2004. Relaxed Eddy Accumulation system for size-resolved aerosol particle flux measurements. *J. Atmos. Oceanic Technol.* **21**, 933–943.

Guenther, A., Baugh, W., Davis, K., Hampton, G., Harley, P., and co-authors. 1996. Isoprene fluxes measured by enclosure, relaxed eddy

accumulation, surface layer gradient, mixed layer gradient, and mixed layer mass balance techniques. *J. Geophys. Res.* **100**, 18555–18567.

Haapanala, S., Rinne, J., Pystynen, K. -H., Hellén, H. and Hakola, H. 2006. Measurements of hydrocarbon emissions from a boreal fen using REA technique. *Biogeosciences* **3**, 103–112.

Held, A., Nowak, A., Wiedensohler, A. and Klemm, O. 2006. Field measurements and size-resolved model simulations of turbulent particle transport to a forest canopy. *J. Aerosol Sci.* **37**, 786–798.

Kulmala, M., Hämeri, K., Aalto, P. P., Mäkelä, J. M., Pirjola, L. and co-authors. 2001. Overview of the international project on biogenic aerosol formation in the boreal forest (BIOFOR). *Tellus* **53B**, 324–343.

Laakso, L., Grönholm, T., Rannik, Ü., Kosmale, M., Fiedler, V. and co-authors. 2003. Ultrafine particle scavenging coefficients calculated from 6 years field measurements. *Atm. Env.* **37**, doi:10.1007/s11270-005-9018-5.

Nho-Kim, E. -Y., Michou, M. and Peuch, V. -H. 2004. Parameterization of size-dependent particle dry deposition velocities for global modeling. *Atm. Env.* **38**, 1933–1942.

Rannik, Ü. 1998. On the surface layer similarity at a complex forest site. *J. Geophys Res.* **28**, 8685–8697.

Rannik, Ü., Petäjä, T., Buzorius, G., Aalto, P., Vesala, T. and co-authors. 2001. Deposition velocities of nucleation mode particles into a Scots pine forest. *Environ. Chem. Phys.* **22**, 97–102.

Rannik, Ü., Aalto, P., Keronen, P., Vesala, T. and Kulmala, M. 2003. Interpretation of aerosol particle fluxes over a pine forest: Dry deposition and random errors. *J. Geophys. Res.* **108** (D17), AAC 3-1-3-11.

Ruijgrok, W., Tieben, H. and Eisinga, P. 1996. The dry deposition of particles to a forest canopy: A comparison of model and experimental results. *Atmos. Environ.* **31**, 399–415.

Sehmel, G. A. 1980. Particle and gas dry deposition: a review. *Atmos. Environ.* **14**, 983–1011.

Seinfeld, J. H. and Pandis, S. N. 1998. *Atmospheric Chemistry and Physics: From Air Pollution to Climate Change*, John Wiley & Sons, Inc., New York.

Slinn, W. G. N. 1977. Some approximations for the wet and dry removal of particles and gases from the atmosphere. *Water Air Soil Poll.* **7**, 513–543.

Vesala, T., Haataja, J., Aalto, P., Altimir, N., Buzorius, G. and co-authors. 1998. Long-term field measurements of atmosphere-surface interactions in boreal forest ecology, micrometeorology, aerosol physics and atmospheric chemistry. *Trends Heat Mass Momentum Transf.* **4**, 17–35.

Zhang, L., Gong, S., Padro, J. and Barrie, L. 2001. A size-segregated particle dry deposition scheme for an atmospheric aerosol module. *Atmos. Environ.* **35**, 549–560.